CHEMISTRY

SYNTHESIS AND CHARACTERIZATION OF NOVEL, METAL-RICH ROOM TEMPERATURE IONIC LIQUIDS AND

COMPUTATIONAL MODELING OF ^{23}Na NMR SHIFTS OF ORGANOMETALLIC COMPOUNDS

C. HEATHER MCMILLEN

Thesis under the direction of Professor Timothy P. Hanusa

ABSTRACT A

A series of room temperature ionic liquids (RTILs) containing MX_4^{2-} (where M = Co, Ni and X = Cl, I) as the counterion have been synthesized from alkyl imidazolium chlorides and the appropriate MX_2 species. A secondary series of RITLs in which the imidazolium cation has been replaced by trihexyl(tetradecyl)phosphonium chloride is also introduced. These salts are liquid at ambient temperatures (ca. 20 °C) and deep blue in color. The thermal behavior and decomposition products of these salts have been probed and provide new synthetic routes to nanoparticulate materials. Also presented is their entrapment in silica matrices to form ionogels and introductory probes into their electrochemical behavior.

ABSTRACT B

Computational modeling was carried out on a variety of ^{23}Na organometallic compounds. Geometry optimization was carried out with DFT calculations in the *Gaussian 03W* suite of programs. The gauge-including atomic orbital (GIAO) method was then used to calculate their ^{23}Na NMR magnetic shielding values. It was determined that the chemical shift of unsubstituted $Na(C_3H_5)$ was very sensitive to the presence of coordinated THF (20 ppm upfield shift). The addition of silyl groups to the allyl has an even larger effect (30 ppm). This is in contrast with NaCp, where coordinated THF causes only a 4 ppm upfield shift.

Approved: Timothy P. Hanusa

SYNTHESIS AND CHARACTERIZATION OF NOVEL, METAL-RICH ROOM TEMPERATURE IONIC LIQUIDS AND COMPUTATIONAL MODELING OF ^{23}Na NMR SHIFTS OF ORGANOMETALLIC COMPOUNDS

By

C. Heather McMillen

Thesis

Submitted to the Faculty of the

Graduate School of Vanderbilt University

in partial fulfillment of the requirements

for the degree of

MASTER OF SCIENCE

in

Chemistry

December, 2010

Nashville, Tennessee

Approved:

Timothy P. Hanusa

Charles M. Lukehart

ACKNOWLEDGEMENTS

I would like to thank the following people:

Dr Timothy P. Hanusa for allowing me the opportunity to conduct research on this project.

Professors Charles Lukehart, David Wright and Bridget Rogers, for their additional help and support.

Dr. Brian Huffman, Brian Hickson and Brian Turner for assisting me in my thermogravametric analyses.

Leslie Hyatt and Jennifer Merritt for assisting me in my Electrochemical Analysis.

James McBride for his training and assistance in obtaining Transition Electron Microscope data.

Funding for this work was provided by several Teaching Assistantships from Vanderbilt University, grants from the Petroleum Research Fund and the GAANN fellowship.

TABLE OF CONTENTS

LIST OF TABLES

LIST OF FIGURES

PART A

SYNTHESIS AND CHARACTERIZATION OF NOVEL, METAL-RICH ROOM TEMPERATURE IONIC LIQUIDS

INTRODUCTION

In recent years, the chemistry of room temperature ionic liquids (RTILs) has rapidly expanded as they have become better understood and their use more prevalent in academic and commercial settings.[1] They possess unique chemical properties, such as large liquid temperature ranges, negligible vapor pressure, and variable pH. They are highly polar non-coordinating solvents whose properties can be fine-tuned in myriad ways. RTILs have been utilized in catalysis,[2] electrochemistry,[3-5] and as designer solvents.[6-8] Metal-containing anions have been incorporated into these ionic liquids, some of which can be air and moisture stable. Many of the metal anions used form the compounds $[MCl_n]^{\gamma-}$, where M is a metal such as Zn, Sn, Fe, Ln, etc.[9, 10] The properties of nickel-based anions in ionic liquids have been explored in several studies.[11] It was found that in several haloaluminate melts an equilibrium existed between $AlCl_4$ and the dimer, $[Al_2Cl_7]^-$. This equilibrium leaves a free chlorine anion, which can be used to complex with nickel(II). The electrochemical behavior of the new species was explored and the standard potential of the species was found to be E_0 = 1.433 V (at 175 °C, versus an Al standard). Furthermore, the existence of similar species, such as the cobalt analog, was explored by Oye and Gruen.[12] In contrast, in these studies the metal chloride anion was present in only very small quantities, and was not considered the predominant anionic species.

RTILs with metal halides as the predominant anion were examined by Seddon in 1996[13] and in previous work by this group in 2009.[14]

Pnictogen compounds of transition metals have been the focus of many recent studies. They have been found to be useful for their magnetic and catalytic properties[15, 16] as well as in thin films.[17] They are also currently being explored for their possible uses in data storage devices.[18] However, synthesis of these compounds can be somewhat problematic. For instance, phosphide compounds were commonly produced by direct reaction of highly toxic nanocrystals using cobalt dichloride and white phosphorous as starting materials.[15] These nanocrystals proved to be useful for the photo-catalytic degredation of various organic dyes.

This work investigates the synthesis of ionic liquid species and their thermal decomposition behavior. Due to their well-understood properties, the dianonic species $NiCl_4^{2-}$ and $CoCl_4^{2-}$ were chosen to be the primary anions of investigation.[11, 12]

EXPERIMENTAL

General Considerations

Commercial ionic liquids were purchased from Strem and Acros. All other reagents were purchased from Aldrich or Fluka and used as received.

Elemental analyses were performed by the University of Illinois Microanalytical Laboratory, Desert Analytics (Tucson, AZ), or at the Micro-Mass Facility, University of California, Berkeley (Berkeley, CA). NMR spectra were taken on a Bruker 400 MHz NMR. Thermogravimetric analyses (TGA) were run on an Instrument Specialist's TGA-1000. Thermal decomposition of bulk ionic liquids was carried out in a Lindberg/Blue tube furnace. Transmission Electron Microscopy images were taken on a Philips CM20 Transmission Electron

Microscope. All electrochemical measurements were conducted using a CHI 660a potentiostat from CH Instruments (Austin, TX). The electrochemical cell was used in a three-electrode configuration with 1.5 mm Pt disc working electrode, Ag wire reference electrode, and a 0.5 mm platinum disc counter electrode. The working and counter electrodes were sealed in epoxy on a resin surface. The surface of the disc electrodes was polished with 3 micron Buehler Metadi II Diamond Polishing Compound.

Synthesis of Parent Ionic Liquids

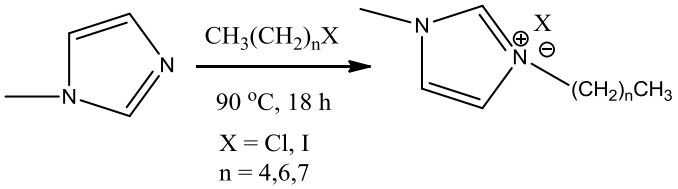

Figure A.1 Synthetic pathway of parent compounds.

1-pentyl-3-methylimidazolium chloride, [C_5mim]Cl. *N*-methylimidazole (4.9 g, 59.8 mmol) and 1-chloropentane (6.3 g, 59.4 mmol) were placed in a 50 mL round bottom flask equipped with a magnetic stirring bar. The mixture was heated to 95 ºC with stirring for 18 h. The resulting yellow liquid was washed with Et_2O (3 x 30 mL) and heated to 100 ºC under dynamic vacuum for 1.5 hours. (9.9 g, 88%)

1-heptyl-3-methylimidazolium chloride, [C_7mim]Cl.

1-chloroheptane (21.12 g, 156.9 mmol) and *N*-methylimidazole (12.36 g, 150.5 mmol) were placed in a 50 mL round bottom flask equipped with a magnetic stirring bar. The mixture was heated to 95 °C with stirring for 20 h. The resulting yellow-orange liquid was washed with Et_2O (3 x 30 mL) and heated to 100 ºC under dynamic vacuum for 1.5 h. Yield was near quantitative.

1-heptyl-3-methylimidazolium iodide, [C_7mim]I.

1-iodoheptane (12.35 g, 54.62 mmol) was treated as for 1-chloroheptane to yield a red liquid in quantitative yield.

1-octyl-3-methylimidazolium chloride, [C_8mim]Cl.

1-chlorooctane (22.38 g, 150.5 mmol) was treated as 1-chloroheptane to yield the product as a yellow liquid in quantitative yield.

1-benzyl-3-methylimidazolium chloride, [Armim]Cl.

Benzyl chloride (8.23 g, 65.0 mmol) was treated as for 1-chloroheptane to yield the product as a yellow liquid in quantitative yield.

Synthesis of Metal Containing Ionic Liquids

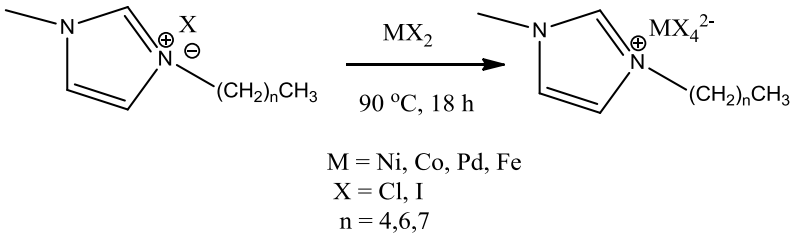

Figure A.2 Synthetic pathway of metal containing imidizolium species.

Bis(1-pentyl-3-methylimidazolium) tetrachloronickelate(II), [PentMeIm]$_2$[NiCl$_4$]. 1-pentyl-3-methylimidazolium chloride (5.26 g, 27.9 mmol) and $NiCl_2(H_2O)_6$ (3.31 g, 13.9 mmol) were placed in a 50 mL round bottom flask equipped with a magnetic stirring bar. The flask was flushed with N_2 and the reaction was allowed to stir at 80 °C for 18 h. The reaction was removed from heat and allowed to cool to room temperature. The solution was dried under vacuum at 95 °C to afford a dark blue liquid (6.24 g, 88%). Anal. Calcd for $C_{18}H_{34}Cl_4N_4Ni$: C, 42.64; H, 6.76; N, 11.05. Found: C, 39.31; H, 6.38; N, 10.19. The empirically found C:H:N values are in the molar ratio 18.0 : 34.8 : 4.0, suggesting that combustion was incomplete.

Bis(1-hexyl-3-methylimidazolium) tetrachloronickelate(II), $[C_6mim]_2[NiCl_4]$.

1-hexyl-3-methylimidazolium chloride (4.29 g, 19.8 mmol) and $NiCl_2(H_2O)_6$ (2.35 g, 9.89 mmol) were placed in a 100 mL round bottom flask equipped with a magnetic stirring bar. The flask was flushed with N_2 and the reaction was allowed to stir at 80 °C for 17 h. The reaction was removed from heat and allowed to cool to room temperature. The solution was dried under vacuum at 95 °C to afford a dark blue liquid in 83% yield. Anal. Calcd for $C_{22}H_{42}Cl_4N_4Ni$: C, 46.92; H, 7.53; N, 9.95. Found: C, 46.04; H, 7.57; N, 9.80.

Bis(1-heptyl-3-methylimidazolium) tetrachloronickelate(II), $[C_7mim]_2[NiI_4]$.

1-heptyl-3-methylimidazolium iodide (5.37 g, 17.4 mmol) and $NiI_2(H_2O)_6$ (3.58 g, 8.51 mmol) were treated as for $[C_7mim]_2[NiCl_4]$. The solution was dried under vacuum at 100 °C to afford a dark red liquid in quantitative yield.

$[C_4mim][C_6mim][NiCl_4]$.

1-butyl-3-methylimidazolium chloride (2.25 g, 12.9 mmol), 1-hexyl-3-methylimidazolium chloride (2.61 g, 12.9 mmol), and $NiCl_2(H_2O)_6$ (3.06 g, 12.9 mmol) were placed in a 100 mL round bottom flask equipped with a magnetic stirring bar. The flask was flushed with N_2 and the reaction was allowed to stir at 90 °C for 23 h. The reaction was removed from heat and allowed to cool to room temperature. The solution was dried under vacuum at 100 °C to afford a dark blue liquid (5.97 g, 91%).

Bis(1-octyl-3-methylimidazolium) tetrachloronickelate(II), $[C_8mim]_2[NiCl_4]$.

1-octyl-3-methylimidazolium chloride (4.54 g, 19.7 mmol) and $NiCl_2(H_2O)_6$ (2.34 g, 9.84 mmol) were treated as for $[C_7mim]_2$[NiCl4]. The solution was dried under vacuum at 90 °C for 2 h to afford a dark blue liquid (5.17 g, quantitative). Anal. Calcd for $C_{24}H_{46}Cl_4N_4Ni$: C, 48.72; H, 7.84; N, 9.48. Found: C, 47.91; H, 7.90; N, 9.38.

Bis(1-benzyll-3-methylimidazolium) tetrachloronickelate(II), [Armim]$_2$[NiCl$_4$].

1-benzyl-2-methylimidazolium chloride (2.17 g, 10.4 mmol) and $NiCl_2(H_2O)_6$ (2.52 g, 10.6 mmol) were treated as for [C_8mim]$_2$[$NiCl_4$]. The resulting dark blue liquid was obtained in quantitative yield.

Bis(1-octyl-3-methylimidazolium) tetrachlorocobaltate(II), [C_8mim]$_2$[$CoCl_4$].

1-octyl-3-methylimidazolium chloride (9.54 g, 41.3 mmol) and $CoCl_2(H_2O)_6$ (4.92 g, 20.7 mmol) were treated as for [C_8mim]$_2$[$NiCl_4$]. The resulting dark blue liquid was obtained in quantitative yield.

Bis(1-heptyl-3-methylimidazolium) tetrachloropalladate(II) [C_6mim]$_2$[$PdCl_4$].

1-heptyl-3-methylimidazolium chloride (4.72 g, 21.8 mmol) and $P1Cl_2$ (1.93 g, 10.9 mmol)were placed in a 100 mL round bottom flask equipped with a magnetic stirring bar. The flask was allowed to stir at 90 °C for 18 h. The reaction was allowed to cool to room temperature. The solution was dried under vacuum at 110 ºC to afford a maroon solid in quantitative yield. Anal. Calcd for C22H42Cl4N4Pd: C, 43.63; H, 6.77; N, 11.05. Found: C, 39.31; H, 6.38; N, 10.19.

Bis(1-hexyl-3-methylimidazolium) tetrachloroferrate(II), [C_6mim]$_2$[$FeCl_4$].

1-hexyl-3-methylimidazolium chloride (4.82 g, 22.2 mmol) and anhydrous $FeCl_2$•$4H_2O$ (2.22 g, 11.2 mmol) were placed in a 50 mL round bottom flask equipped with a magnetic stirring bar. 20 mL of acetonitrile was added, and the mixture was stirred for 1 h. The reaction was placed on a Schlenk line and heated under dynamic vacuum (75 °C, 18 h) to afford a red liquid in quantitative yield.

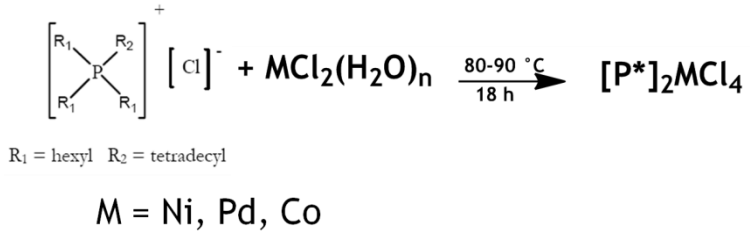

Figure A.3 Synthetic pathway of metal containing phosphonium species.

Bis(trihexyl(tetradecyl)phosphonium) tetrachloronickelate(II), $[P^*]_2[NiCl_4]$.

Trihexyl(tetradecyl)phosphonium chloride (P*Cl, 2.51 g, 4.85 mmol) and $NiCl_2(H_2O)_6$ (0.58 g, 2.42 mmol) were treated as for $[C_8mim]_2[NiCl_4]$. The resulting dark blue liquid was obtained in quantitative yield.

Preparation of Iono-gels

Bis(trihexyl(tetradecyl)phosphonium) tetracobaltate(II), $[P^*]_2[CoCl_4]$.

Trihexyl(tetradecyl)phosphonium chloride (17.16 g, 33.0 mmol) and $CoCl_2(H_2O)_6$ (3.94 g, 16.5 mmol) were treated as for $[C_8MIM]_2[NiCl_4]$. The resulting dark blue liquid was obtained in quantitative yield.

Acid Catalyzed preparation of Bis(trihexyl(tetradecyl)phosphonium) $[NiCl_4]$ ionogel

1.61 g $[P^*]_2[NiCl_4]$ (1.38 mmol) was added to a beaker with 3.51 g of TMOS (23.05 mmol) and 3.66 g MTMS (26.87 mmol). The solution was exposed to sonication until the system became homogenous. Next, 0.5 mL of formic acid was added to the solution. The system was allowed react under sonication for 8 h. The thickened solution was allowed to set and age. The system shrank slightly and the final gel was a mint green cracked solid. This solid was placed in a 100 °C oven to remove any associated water and turned a royal blue color.

Base Catalyzed preparation of Bis(trihexyl(tetradecyl)phosphonium) [$NiCl_4$] ionogel

$[P^*]_2[NiCl_4]$ (0.291 g, 0.25 mmol) was added to a beaker with TMOS (0.796 g, 5.23 mmol), Methyltrimethoxysilane (MTMS, 0.704 g, 5.15 mmol) and 1 mL ethanol. Two drops of concentrated ammonium hydroxide was added to catalyze the system. The solution was stirred rapidly until a blue power formed. This powder was dried in a 100 °C oven and then ground in a mortar.

Base Catalyzed preparation of Bis(trihexyl(tetradecyl)phosphonium) [$CoCl_4$] ionogel

$[P^*]_2[CoCl_4]$ (0.146 g, 0.12 mmol) was added to a beaker with TMOS (0.320 g, 2.10 mmol), MTMS (0.322 g, 2.37 mmol) and 1 mL ethanol. Two drops of concentrated ammonium hydroxide was added to catalyze the system. The solution was stirred rapidly until a blue power formed. This powder was dried in a 100 °C oven and then ground in a mortar.

RESULTS AND DISCUSSION

Synthesis of Metal Containing Ionic Liquids

In previous work, RTILs have been prepared containing a variety of MCl_4 anions (where M = Fe, Ni, Zn, Mn).[14, 19] Nickel was chosen as the metal of choice for continuing investigation and a variety of chain lengths were explored for the functionalization of the imidazolium cation (See Figure 1). The syntheses were not without some difficulty, as the pentyl derivative ($[C_5mim]_2[NiCl_4]$) was found to gel occasionally if the system was overheated, making it difficult to work with. However, the other two nickel species were both liquid at room temperature, in contrast to some other ionic liquids which have to be warmed up slightly before melting occurs. Also, the iron derivative ($[C_7mim]_2[FeCl_4]$) was found to deposit an orange precipitate after several days; it may be an iron oxide, but this has not yet been further investigated. The

palladium derivative ($[C_7mim]_2[PdCl_4]$) initially formed a dark garnet-colored liquid, and upon standing, solidified into a dark brown-red solid. It is thought that this is due to the planar nature of the $PdCl_4^{2-}$ anion. This planar character allows for a more efficient degree of packing, something not allowed by the tetrahedral shape of the other anions.

The RTILs previously prepared by Meredith et al. containing iron, zinc, and manganese all had acceptable elemental analyses.[19] However, some difficulty was seen with the elemental analysis of the nickel compounds. Typically, the carbon and hydrogen percentages were a bit low, indicating an incomplete combustion of the materials in the analysis procedure. It is presumed that upon analysis, the species form side products that are not detectable in the combustion process.

The imidazolium cation is somewhat problematic in that it is hygroscopic; excess water causes the $NiCl_4^{2-}$ cation to dissociate into $NiCl_2$ and Cl^-. (Note: The addition of water is completely reversible, and is easily removed under heat or vacuum, as seen in Figure A.4.) The trihexyl(tetradecyl)-phosphonium cation was introduced to provide an alternative to imidazolium as it is not hygroscopic. Cobalt and nickel were the metals of choice as they have been previously studied in RTILs[11, 12] and the ionic salts synthesized here are liquid at room temperature.

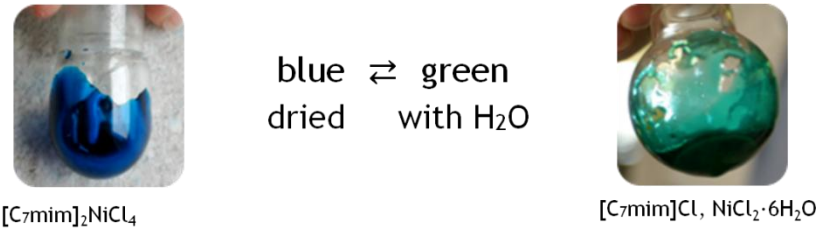

Figure A.4 Hygroscopic behavior of imidazolium species.

Viscosity Comments

The viscosity of RTILs tend to vary drastically from about 18-1100 cP or more (8,10). The nickel ionic liquids discussed here typically have a viscosity of 110-180 cP at room temperature. Their viscosities were measured previously[14] from approximately 23–60 °C. (Figure A.5) A representative sample of viscosities, including representative samples of analogous $[BF_4]^-$ and $[PF_6]^-$ compounds, is presented in Table A.1 The two longer-chained salts ($[C_7mim]^+$ and $[C_8mim]^+$ cations) have higher viscosities than do those with shorter chains. Below 30 °C, the viscosity of the mixed species ($[C_4mim][C_6mim][NiCl_4]$ which could be considered to have an ''average" chain length of C_5) tracks closely with that of the single-chained $[C_5mim]_2[NiCl_4]$ salt. Above 30 °C, the viscosities start to diverge, and values for the mixed imidazolium salt stay roughly 15% below that of the single. The effect of mixed cations on the viscosities of ionic liquids is not well studied (cf. the relative rarity of viscosity measurements in systems with mixed anions[9, 20, 21]), so that it is not clear how typical the behavior of $[C_4mim][C_6mim][NiCl_4]$ is.

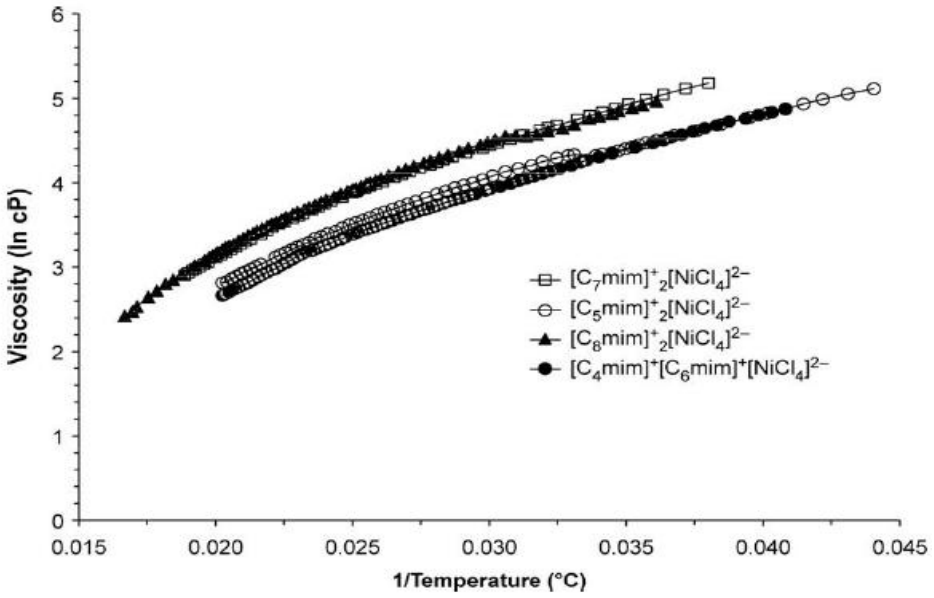

Figure A.5 Viscosity behavior of imidazolium parent compounds.

The salts containing the $[NiCl_4]^{2-}$ anion seem to have considerably lower viscosities than the analogous $[PF_6]^-$ salts and similar viscosities to the $[BF_4]^-$ species.[22, 23] The similarity of viscosity is somewhat surprising due to the fact that the higher charge on the $[NiCl_4]^{2-}$ anion would be expected to strengthen the coulombic attractions between the ionic species. This would, in turn, increase the viscosity of the species. However, this seems to be counteracted by the larger radius of the $[NiCl_4]^{2-}$ cation (with effective radii of ca. 2.9 Å versus 2.1 Å, respectively)[24] which serves to weaken the interactions between the cation and anion, and this compensate for the higher charge. Also, the viscosity of the mixed species, $[C_4mim][C_6mim][NiCl_4]$, is comparable to that of $[C_4mim][BF_4]$. This further underscores the potential of mixed cationic species to lower viscosities.

Table A.1 Representative values for substituted imidazolium salts.

Ionic Liquid	T (°C)	η (cP)	Ref
$[C_5mim]_2[NiCl_4]$	24.9	125	14
$[C_5mim]_2[NiCl_4]$	30.2	76	14
$[C_5mim]_2[NiCl_4]$	40.2	33	14
$[C_7mim]_2[NiCl_4]$	26.3	178	14
$[C_7mim]_2[NiCl_4]$	30.1	116	14
$[C_7mim]_2[NiCl_4]$	40.0	49	14
$[C_8mim]_2[NiCl_4]$	27.7	144	14
$[C_8mim]_2[NiCl_4]$	30.2	109	14
$[C_8mim]_2[NiCl_4]$	40.0	50	14
$[C_8mim][PF_6]$	30.0	452	22
$[C_8mim][BF_4]$	30.0	82	23
$[C4mim][C_6mim][NiCl_4]$	25.1	122	14
$[C4mim][C_6mim][NiCl_4]$	30.0	70	14
$[C4mim][C_6mim][NiCl_4]$	40.0	30	14
$[C_4mim][PF_6]$	30.0	204	22
$[C_4mim][BF_4]$	30.0	91.4	22
$[C_6mim][PF_6]$	30.0	363	22
$[C_6mim][BF_4]$	30.0	177	22

Plots of the complete data sets (Figure A.5) indicate slightly non-Arrhenius behavior for the ionic liquids at higher temperatures. Nevertheless, a fit of the data to an Arrhenius-like equation that expresses the energy of activation for viscous flow, $\eta = \eta_0 e^{E\eta/RT}$, for which Eη is the energy of action for viscous flow, and η_0 is a constant, is very good for all four liquids ($r^2 > 0.99$). The Eη values (Table A.2) cluster around 65–69 kJ mol-1, without an obvious correlation with the chain length. These are near the value of 55.7 kJ mol^{-1} determined for the RTIL [choline][Zn_2Cl_5][9, 25], but are roughly four times higher than the average of 17 ± 3 kJ mol^{-1} found for various RTILs with more common anions ($[BF_4]^-$, $[PF_6]^-$, $[Tf_2N]^-$, $[Tf_2C]^-$), even when the cations are hydroxy-substituted, and thus capable of engaging in hydrogen bonding.[25]

Table A.2 Energy of activation for viscous flow of tetrachloronickelate salts.

Compound	Eη (kJ mol^{-1})	r^2
$[C_5mim]_2[NiCl_4]$	65.8	0.997
$[C_7mim]_2[NiCl_4]$	67.8	0.998
$[C_8mim]_2[NiCl_4]$	64.6	0.995
$[C_4mim][C_6mim][NiCl_4]$	68.7	0.996

Thermal Behavior

$[C_7mim]_2[NiCl_4]$, $[C_7mim]_2[NiI_4]$, $[P^*]_2[NiCl_4]$ and $[Armim]_2[NiCl_4]$.

The decomposition of imidazolium salts is heavily influenced by the identity of the anion. For instance, $[C_1mim][PF_6]$ decomposes in a single step but $[C_1mim][BF_4]$ does so in several steps.[18] Thermal decomposition was carried out for all of the species. The resulting TGA analysis for $[C_7mim]_2[NiCl_4]$ is shown in Figure 1.6. The first decomposition step begins at around 305 °C and the second starts at 430 °C. Decomposition is completed near 700 °C, with a residual mass of 14%. This mass does not correspond to the presence of completely reduced nickel metal or nickel chloride. To further explore this point, a sample of $[C_7mim]_2[NiCl_4]$ was

placed in a tube furnace at 700 °C for 30 min under N_2. After cooling, powder XRD was run on the decomposition product, and indicated the presence of both elemental nickel and nickel chloride. Given this information, the residual weight in the TGA experiment corresponds to a $Ni:NiCl_2$ ratio of 3:1.

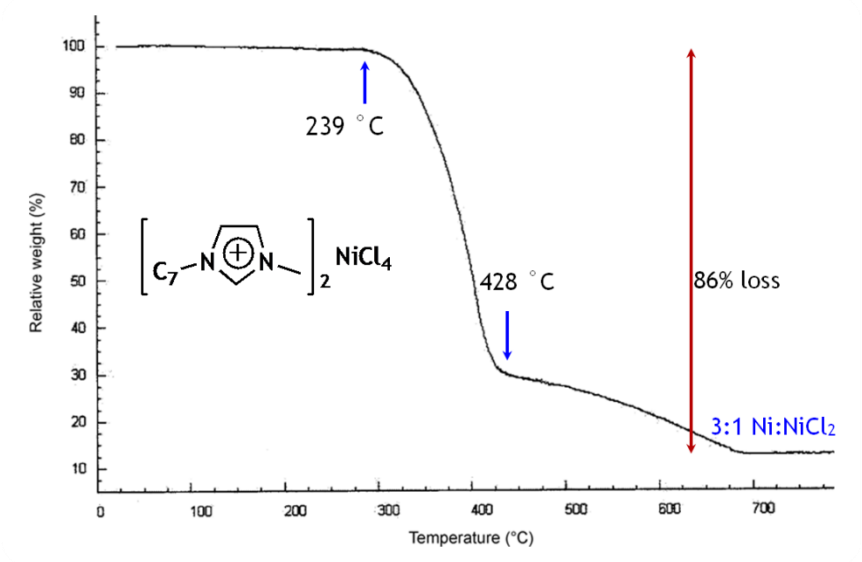

Figure A.6 Thermal decomposition process for $[C_7mim]_2[NiCl_4]$ under N_2.

Similar analyses were run for $[C_7mim]_2[NiI_4]$. Powder XRD analysis (Figure A.7) run on the decomposition product showed the presence of elemental nickel alone. A Scherrer analysis of peak widths suggested an average particle size of 44 nm.

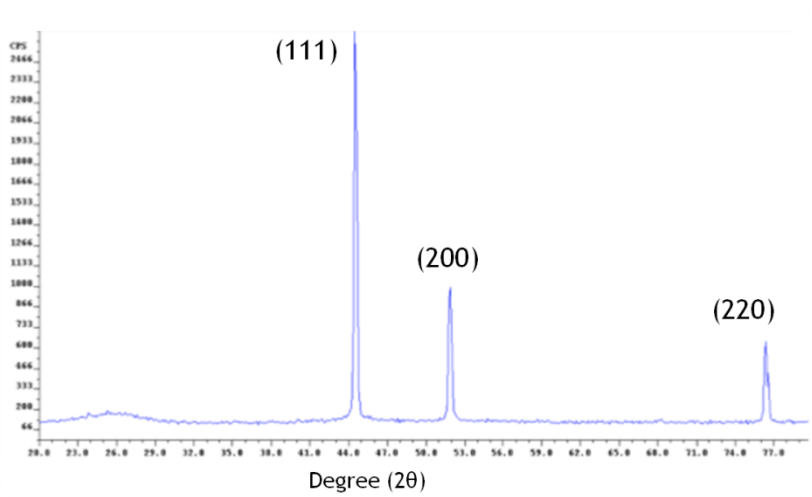

Figure A.7 Thermal Decay Product for $[C_7mim]_2[NiI_4]$ Under N_2.

The thermal decomposition of $[Armim]_2[NiCl_4]$ under nitrogen gas occurs in four total steps (Figure A.8). The first step begins around 213 °C and the final step ends around 580 °C. The total loss of mass indicates the presence of nickel metal. Also, the parent compound, [Armim]Cl, was unsuccessfully investigated for use as a MALDI matrix.

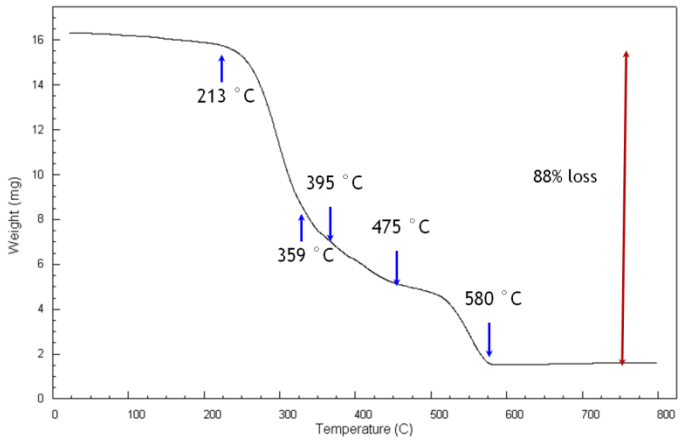

Figure A.8 Thermal decomposition process for $[Armim]_2[NiCl_4]$ under N_2.

The thermal decomposition of $[P^*]_2[NiCl_4]$ under nitrogen gas is carried out from 300–400 °C and occurs in a single step (Figure A.9), as expected for imidazolium and phosphonium

based RTILs.[14] Analysis of the curve reveals that the salt does not decompose cleanly into nickel metal.

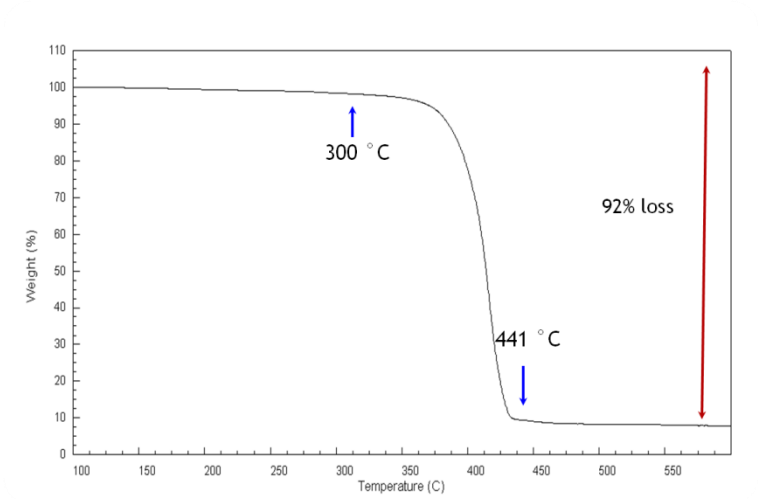

Figure A.9 Thermal Decomposition of $[P^*]_2[NiCl_4]$ under N_2.

$[C_8mim]_2[CoCl_4]$ and $[P^*]_2[CoCl_4]$

The thermal degradation of both $[C_8mim]_2[CoCl_4]$ and $[P^*]_2[CoCl_4]$ begin at about 285 °C and ends at around 600 °C. The TGA of $[P^*]_2[CoCl_4]$ is similar to the analogous nickel salt. Figure A.10 shows the powder XRD of the decomposition product for $[P^*]_2[CoCl_4]$. This overlays quite nicely with the expected XRD results for Co_2P. Co_2P is a semiconductor and a substance of interest in catalysis[26] and corrosion resistant coatings.[27]

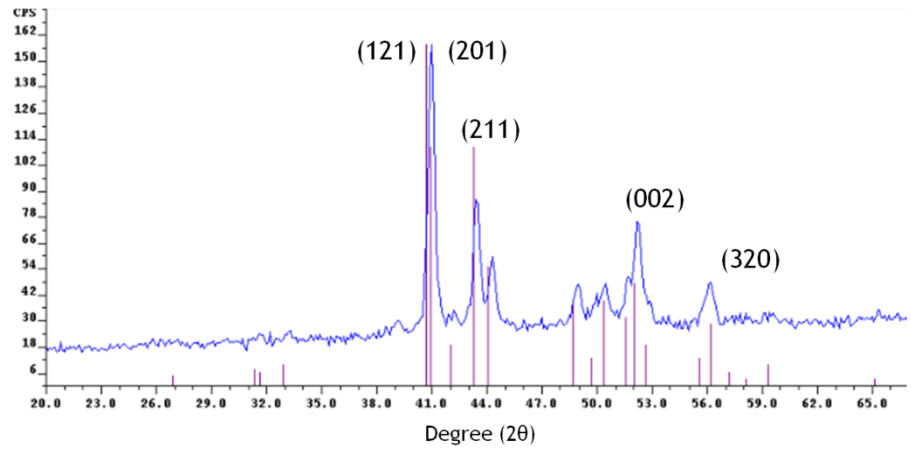

Figure A.10 Thermal Decay Product for $[P^*]_2[CoCl_4]$ under N_2.

The powder XRD of the decomposition product for $[C_8mim]_2[CoCl_4]$ is shown in Figure 1.11 a-b. In Figure 11a, the XRD scan has been overlayed with the expected XRD output for fcc cobalt metal, in 11b, the overlay for hcp cobalt has been added. Both agree quite well with the shown peaks. Such a mixture of packing arrangements can be expected to form around 800 °C, the temperature at which the largest part of the decomposition was carried out.

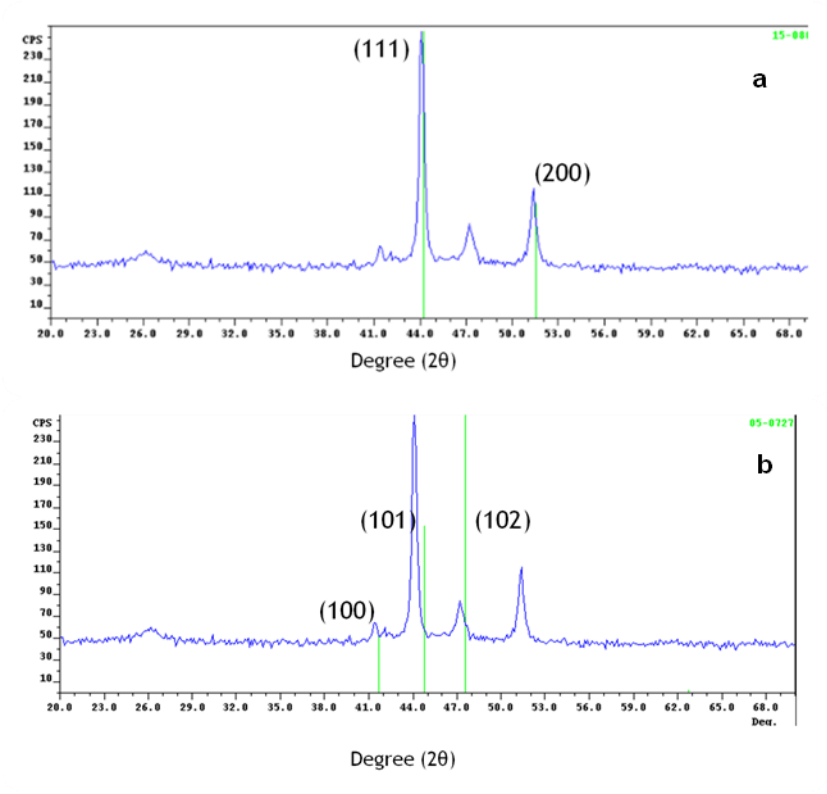

Figure A.11 Thermal decay products of $[C_7mim]_2[CoCl_4]$ under N_2 (a) fcc cobalt (b) hcp cobalt.

$[C_7mim]_2[PdCl_4]$, $[P^*]_2[PdCl_4]$ and $[C_7mim]_2[FeCl_4]$

The decomposition of the palladium salt analogous to $[C_7mim]_2[NiCl_4]$ follows the same basic pattern, but at a slightly higher temperature (500−625 °C as opposed to the 300−425 °C decomposition observed in the nickel species). The preparation of $[P^*]_2[PdCl_4]$ resulted in a blood-red liquid that decayed in a similar fashion to the analogous nickel salt. The iron salt begins its decomposition at an even lower temperature, but loses its ligands in a total of three steps. The first is between 275 and 375 °C, the second from 375−450 °C and the final decomposition step is from 450−550 °C (Figure A.12). Analysis of both of these scans suggests a mixture of metal and metal chloride as seen in the analogous nickel species.

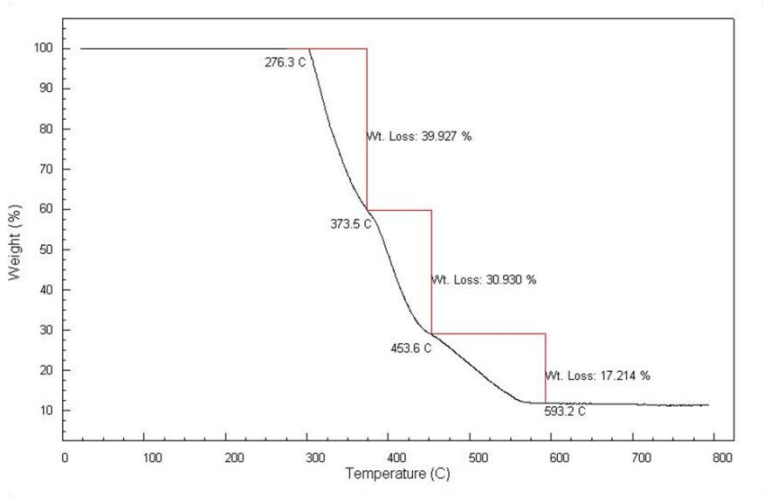

Figure A.12 Thermal decomposition process of $[C_7mim]_2[FeCl_4]$ under N_2.

As the palladium salt is solid at room temperature, a DSC scan was run on the maroon solid (Figure A.13). This scan shows a lattice transformation of 15.6 J/sg at about 75 °C before melting occurs at between about 95−100 °C. The lattice transformation corresponds to a physical change where the solid converts from a dull maroon powder to a rather more vividly maroon gel-like substance.

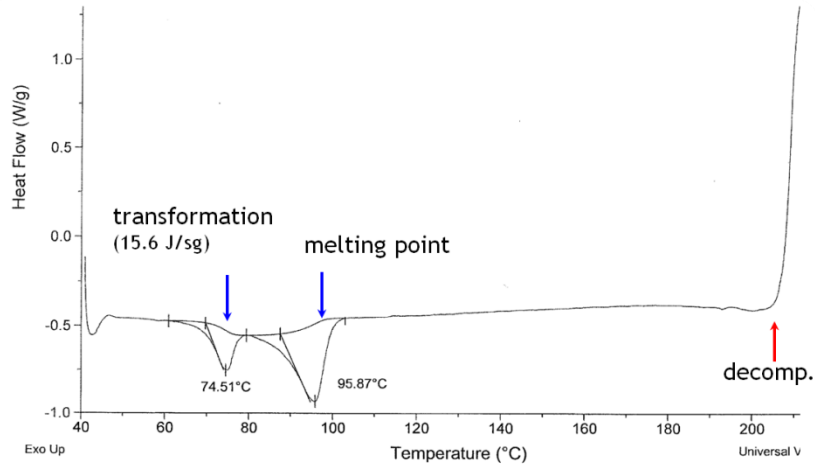

Figure A.13 DSC scan of $[C_7mim]_2[PdCl_4]$.

Electrochemical Behavior

The electrochemical behavior of metals in ionic liquids is a subject of some interest. Discovering a completely reversible redox system is necessary to the development of any probes.[28] Initial cyclic voltammagram (CV) investigations were complicated by the fact that $NiCl_4^{2-}$ tends to dissociate in aqueous media. Therefore, a system was devised to take CVs of the neat ionic liquids. This was done by obtaining a sensor head from multianalyte microphysiometer. (Figure A.14). This probe was inverted and the inlet and outlet holes sealed so that neat ionic liquid could be smeared on the surface.

Figure A.14 Modified Electrochemical Sensor Head.

The CV scans of neat $[C_7mim]_2[NiCl_4]$ show an irreversible oxidation (Figure A.15) This is contrasted with the CV scans of similar cobalt species. For instance, $[C_7mim]_2[CoCl_4]$ shows two irreversible oxidation peaks and the CV of $[P^*]_2[CoCl_4]$ shows a single oxidation peak. None of these are suitable for use in any kind of electrochemical sensor, so more investigation is needed to find a suitable system.

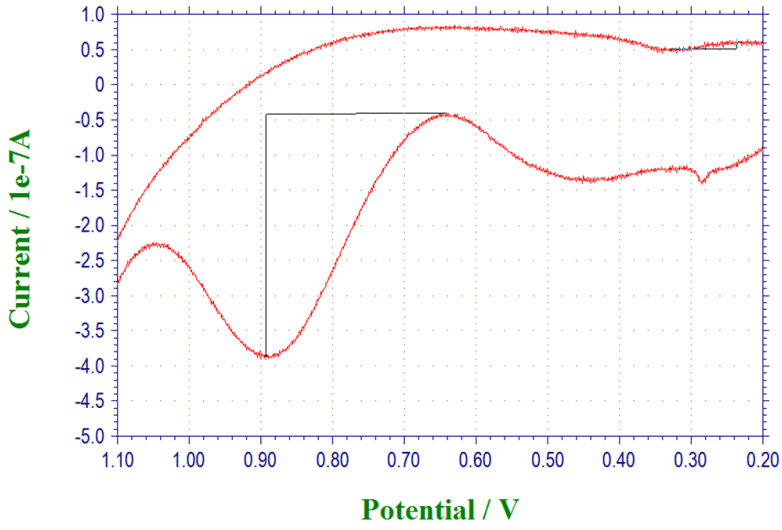

Figure A.15 Electrochemical Behavior of $[C_7mim]_2NiCl_4$.

Iono-gel Preparation

Early attempts at iono-gel synthesis involved acid catalysis of monoliths. The process was extremely long and the resulting solids tended to crack extensively. However, it was noted that the equilibrium between $NiCl_4$ and $NiCl_2$ in the presence of water was maintained as shown in Figure A.16. This is useful as it demonstrates communication between the encapsulated ionic liquid and the outside atmosphere, without allowing the ionic liquid to escape.

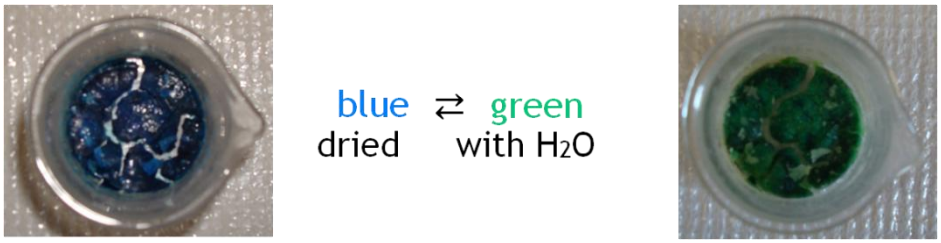

Figure A.16 Hygroscopic Behavior of Imidazolium Species Encased in Silica.

As the ionic liquids are not completely miscible with the silicate solution, separation into phases was a common problem, leading to phased materials instead of the homogenous

monoliths desired. Therefore it was decided to move to base catalysis of powdered ionogels. This method streamlined the ionogel production process, allowing quick and efficient synthesis. TEM analysis of base catalyzed ionogels containing $[P^*]_2[NiCl_4]$ and $[P^*]_2[CoCl_4]$ (Figure A.17) showed amorphous particles with a large size range from about 20 nm to several hundred nanometers. This synthesis offers benefits in that is done in a single step, in contrast to previous work where the sol-gels were synthesized with non-metallic ionic liquids and the metal ions added after the fact by long exposure to sonication.[29]

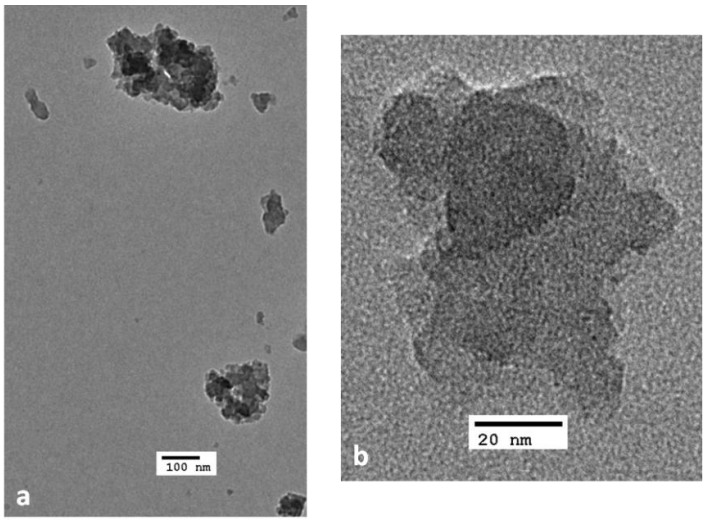

Figure A.17 TEM images of sol-gel encapsulated ionic liquids. a) $[P^*]_2[NiCl]_4$ b) $[P^*]_2[CoCl_4]$.

CONCLUDING REMARKS

The synthesis of RTILs of $NiCl_4^{2-}$ and $CoCl_4^{2-}$ with imidazolium and phosphonium based cations has opened avenues of interest into several areas of research. We have shown that their thermal decomposition products can lead to new synthetic routes to possibly semiconducting nanoparticulate materials. We have also shown that they can be successfully immobilized in silica matrices in a single step. This behavior, coupled with the conductive

properties of these species could lead to the development of new probes for sensor apparatuses.

CHAPTER II

COMPUTATIONAL MODELING OF ^{23}Na NMR SHIFTS OF ORGANOMETALLIC COMPOUNDS

INTRODUCTION

Overview

The study of ^{23}Na NMR has been of great interest in many contexts, from the study of sodium presence and behavior in cheese[30] to how sodium behaves in cancerous cells.[31] This type of investigation is aided by the fact that sodium is a monoisotopic species with I = 3/2 and fairly small shift range (ca. 80 ppm).[32] This shift range can be divided into three major subsets, aqueous sodium (ca. −10 to +20 ppm), organometallic sodium (ca. +30 to −40 ppm) and the sodide anion (−60 ppm and above) . The ^{23}Na nucleus has a receptivity that is 545 times higher than that of ^{13}C, and a high resonance frequency (e.g., 106 MHz at a magnetic field strength of 9.4T (^{1}H = 400 MHz).

Previous studies of ^{23}Na in non-aqueous environments have focused on solid-state NMR chemical shifts with Hartree-Fock and DFT methods[33, 34]; allowing for a better controlled coordination environment around the sodium nuclei. To our knowledge, no computational investigation of ^{23}Na NMR shifts in organic media has been carried out. The object of this paper is to set forth an initial probe into this sphere of investigation.

Relevant Experimental Background

Table B.1 provides a compilation of reported ^{23}Na chemical shifts of both organometallic and, for comparative purposes, some coordination compounds in nonaqueous solvents. The list only hints at some of the potential difficulties in attempts to rationalize chemical shift values.

To begin with, although a sodium chloride solution in H_2O or D_2O is universally used as the standard for ^{23}Na NMR spectroscopy, and 1.0 M is the most commonly encountered concentration, other values that have been used range from saturated solutions (approximately 6.2 M at room temperature) to 0.02 M. In a study published several decades ago, however, Popov *et al.* demonstrated that for a given solvent, providing strong ion pairing was not in play, concentration effects in simple sodium salts were relatively minor.[35] The shift of $Na[BPh_4]$ in THF, for example, varies by less than 0.2 ppm over the concentration range from 0.5–0.125 M.

Temperature effects on shift values and especially line widths can be larger, however; on cooling a methanol solution of $Na[BPh_4]$ from 310K to 210K, the chemical shift moves downfield by 1.5 ppm, but the line width increases from 60 Hz to 330 Hz.[36] Linear correlations between chemical shifts and empirical solvent parameters (e.g., Gutmann's donor numbers[37]) have been observed when it seems likely that the cation is in a solvation cage (e.g., with solutions of $Na[ClO_4]$, $Na[BPh_4]$); that correlation is weaker or nonexistent when contact ion pairing is involved.[35]

Table B.1 Sodium complexes and their corresponding ^{23}Na NMR chemical shifts in nonaqueous media [a]

Compounds	δ_{exp} (ppm)	Solvent (ref.)	Ref.
$Na(MeC_5H_4)$	–36.5	THF–d_8 (1.0 M NaCl)	33
$Na(C_5H_5)$	–33.4	THF–d_8 (1.0 M NaCl)	33
$Na[BPh_4]$ (0.5 M)	–8.12	THF–d_8 (satd. NaCl; *ca*. 6.2 M)	35
$Na[Zn(1,3–(SiMe_3)_2C_3H_3)_3]$	–7.16	THF–d_8 (1.0 M NaCl)	38
$[Na\{C(SiMe_3)Ph_2\}]_n$	–5.4 ($\Delta\nu_{1/2}$ = 500 Hz)	C_6D_6 (1.0 M NaCl)	39
$Na[BPh_4]$ (20 mM)	−3.77	1 : 1 (v/v) $CDCl_3$: CD_3CN) (0.02 M NaCl)	40
$[Na\{C(SiMe_3)Ph_2\}(PMDETA)]$	–3.4 ($\Delta\ \nu_{1/2}$ = 550 Hz)	C_6D_6 (1.0 M NaCl)	39
$Na[1,3–(SiMe_3)_2C_3H_3]$	−3.30	THF–d_8 (1.0 M NaCl)	38
(Na, BPh_4)-calix[4]arene´	−2.11	1 : 1 (v/v) $CDCl_3$: CD_3CN) (0.02 M NaCl)	40
Na^+(*aq*) (1.0 M NaCl)	0.00 (reference)	D_2O	
2–ethylhexyl sodium•NaCl 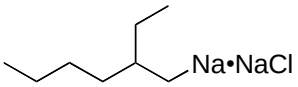	8.1	heptane (10% NaCl; *ca.* 1.7 M)	41
$Na[Zn(1,3–(SiMe_3)_2C_3H_3)_3]$	12.89	C_6D_6 (1.0 M NaCl)	38
2–ethylhexyl sodium 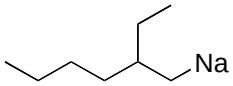	27	heptane (10% NaCl; *ca.* 1.7 M)	41

[a] Abbreviations: calix[4]arene´ = 5,11,17,23–tetra–*tert*–butyl–25,26,27,28–tetrakis(*N*,*N*–diethylaminocarbonyl)methoxy-calix[4]arene, PMDETA = *N*,*N*,*N*´,*N*´,*N*´´-pentamethyldiethylenetriamine, THF = tetrahydrofuran.

Areas of Interest

The data in Table B.1 does suggest a few characteristic regions of interest. Cyclopentadienyl derivatives have strongly upfield resonances, which are undoubtedly related to the Na^+ being in the ring current of the Cp´ ligand; similar influences are known for lithium cyclopentadienides.[42, 43] Other π-bound ligands do not provide the same degree of shielding, as evidenced by the shift of Na[1,3-$(SiMe_3)_2C_3H_3$], some 30 ppm downfield of NaCp. Alkyl groups are not easily characterized; both slightly shielded (Na[C$(SiMe_3)Ph_2$], at δ –5.4 ppm) and strongly deshielded species (2-ethylhexyl sodium, at +27 ppm) are represented. The sensitivity of these shifts to ion pairing is illustrated by the NaCl adduct of 2-ethylhexyl sodium, which is 19 ppm upfield of the parent compound. There is very limited data on solvent effects; Na[Zn(1,3–$(SiMe_3)_2C_3H_3)_3$] displays a downfield shift of 20 ppm in moving from THF to benzene, but this may reflect a substantial change in coordination environment (as observed in the lithium analogue[44]), which is of course affected by the solvent polarity but would not be simply correlated with solvent donor properties. There is not a consistent picture of the role of coordination number in ^{23}Na NMR shifts, as there is in, for example, ^{9}Be or ^{89}Y NMR[45, 46] spectroscopy (i.e., higher coordination numbers leading to more shielding), partially because the exact coordination environments of the sodium ions in solution is difficult to establish. Whether there is such a correlation even in the solid state has been disputed.[47]

COMPUTATIONAL METHODS

Geometry optimization and NMR shielding calculations were performed with the *Gaussian 03W* suite of programs[48] and the GIAO (gauge–including atomic orbitals) method.[49] For geometry optimizations and shielding calculations, the parameter–free PBE1PBE[50] functional

was used; it provides reliable NMR shielding values. The standard 6–311+G(2p,d) basis sets were used for all geometry optimizations and shielding calculations. For the calculations on the aquo ions, an ultrafine grid and DIIS convergence acceleration was used owing to the extremely flat potential energy surfaces involved. The aggregate species, $\{Na(1,3\text{-}(SiH_3)_2C_3H_3)\}_4$, was synthesized by Cameron Gren, and the synthesis outlined in a paper by McMillen et al.[38]

RESULTS AND DISCUSSION

General Considerations

It is imperative to accurately determine the geometries of the selected species in order to maximize the efficacy of the computational process. In order to carry this out, a comparatively high level of theory must be used.[51] Figures B.1-4 and 6-8 contain the geometry–optimized structures and selected bond lengths of the complexes used in this study. The bond distances and angles are reasonable, although exact comparisons with crystallographically determined structures are not usually possible. The Na–O bond distance calculated for the $[Na(thf)_4]^+$ cation, however, precisely matches the 2.301 Å average distance reported for the cation in the crystal structure of tetrakis(tetrahydrofuran)sodium tetrakis(4-methylbenzenecarbodithioato) samarium(III).[52]

Standard Species

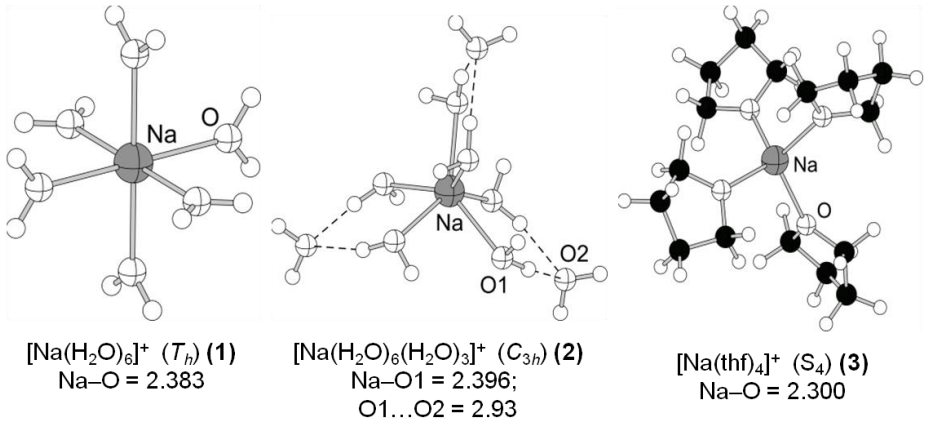

Figure B.1 Optimized structures of standard species.

$[Na(OH_2)_x]_+$: $[Na(OH_2)_6]_+$ (**1**), $[Na(OH_2)_6(OH_2)_3]_+$ (**2**). It is essential to carefully select the choice for modeling the shift reference for any NMR project; if its geometry and shielding value are incorrect, all calculated chemical shifts are affected. This becomes complicated in ^{23}Na NMR as the sodium aquo ion, $[Na(OH_2)_x]^+$, is a somewhat ill-defined species. Hydration numbers from 4–8 have been cited for it.[53-55] The value of *x* (i.e., for the first coordination shell) is commonly taken as approximately 6, for example Waizumi and Fukushima used **1** with T_h symmetry as the reference molecule in a DFT study of cluster models of aquo ions.[56] They noted that this ion was not found to be a minimum, and we confirmed this at the PBE1PBE/6-311+G(2d,p) level (3-fold degenerate frequency at –62 cm^{-1}).

Liu *et al.* have thoroughly discussed the general inadequacy for NMR calculations of a "single shell" ion as a model for $[Na(OH_2)_x]^+$.[57] We accordingly added three additional water molecules to bridge the directly coordinated waters of the T_h structure. It optimized to a geometry of C_{3h} symmetry in which the direct coordination environment of the sodium is trigonal prismatic (**2**). Although it also is not a minimum at the PBE1PBE/6-311+G(2d,p) level (one frequency at –44 cm^{-1}), it maintains a coordination number of 6 for the first "shell" and

adds the beginning of a second coordination sphere around sodium. We deemed this an improvement over the minimal $[Na(OH_2)_6]^+$ ion, and used it as our reference. Interestingly, the calculated isotropic shielding values for **1** and **2** differ by 8.8 ppm, illustrating the sensitivity of calculated shifts to small changes in coordination environment (the Na–O bond distances differ by only 0.013 Å).

A theoretical shift is calculated by subtracting the absolute shielding of a complex from that of a calculated reference. Experimental and predicted ^{23}Na NMR shifts of the complexes studied are listed in Table B.2. As discussed below, the calculated shifts were close enough to the experimental value that scaling methods were not applied.[46, 58, 59]

$[Na(thf)_4]^+$(**3**). The tetrasolvated **3** was used as a likely species for the sodium ion in THF solution.[60-62] Its calculated shift of δ –5.6 ppm is near that observed for several species in THF solution, including $Na[BPh_4]$, $Na[Zn(1,3–(SiMe_3)_2C_3H_3)_3]$, and $Na[1,3–(SiMe_3)2C_3H_3]$, and suggests that these complexes may exist as solvent separated ion pairs in THF.

Table B.2 Predicted shielding constants (σcalc) and chemical shifts (δcalc) in ppm.

Complex	**σcalc**	**δcalc**	**δexp (solvent)**	**Δδ[a]**
$[Na(H_2O)_6(H_2O)_3]^+$ (**2**)	558.01	0.0	0.0[b]	0.0
$[Na(thf)_4]^+$ (**3**)	565.61	–5.6		–
$Na(C_5H_5)$ (**4**)	590.84	–32.8	–33.4 (THF–*d*8)[22]	0.6
$Na(C_5H_5)(thf)$ (**5**)	595.30	–37.3		–3.9
$Na(C_3H_5)$ (**6**)	519.57	38.4	–3.30 (THF–*d*8)[c]	41.7
$Na(C_3H_5)(thf)$ (**7**)	540.99	17.0		20.3
$Na(1,3\text{-}(SiH_3)_2C_3H_3)$ (**8**)	551.46	6.5		9.8
$Na(1,3\text{-}(SiH_3)_2C_3H_3)(thf)$ (**9**)	556.90	1.1		4.4
$\{Na(C_3H_5)\}_4$ (**10**)	575.27	–17.3		–14.0
$\{Na(1,3\text{-}(SiH_3)_2C_3H_3)\}_4$ (**11**)	579.14	–21.1		–17.8
$\{Na(C_3H_5)(thf)\}_4$ (**12**)	572.94 (Na1)	–14.9		–12.5
	574.45 (Na2)	–16.4		–12.8
$Na(C_9H_7)$ (**13**)	603.06	–45.1		N/A
$Na(C_9H_7)(thf)$ (**14**)	589.39	–31.35		N/A
$NaBH_4$ (**15**)	571.42	–13.41		–5.3
$NaB(CH_3)_4$ (**16**)	580.04	–22.0		–13.9
$NaB(CH_3)_4(thf)$ (**17**)	560.20	–2.19		5.9
$Na(BPh_4)$ (**17**)	614.46	–56.5	–8.12 (THF–*d*8)	–48.3
2–ethylhexyl sodium (**19**)	566.04	–8.0	27	35.0
Sodium Adamantazane(**18**)	631.65	–73.63	–61.0[d]	–12.6

[a]Δδ = δcalc – δexp. [b]By definition. [c]This work; the experimental value is for $Na(1,3\text{-}(SiH_3)_2(C_3H_3)(thf)$. [d]solid state

Cyclopentadienyl Species

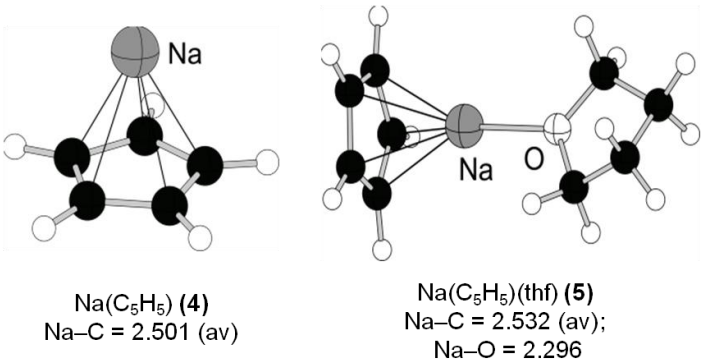

Figure B.2 Optimized structures of cyclopentadienyl species.

Complexes 4,5: $Na(C_5H_5)$ (**4**), $Na(C_5H_5)(thf)$ (**5**). These molecules were included for calibration purposes; the predicted ^{23}Na NMR shift for sodium cyclopentadienide is extremely close to that reported for the compound in THF solution, and the addition of THF causes an upfield shift of less than 5 ppm. This indicates that, as discussed above, the ring current of the Cp´ anion evidently dominates the shift.

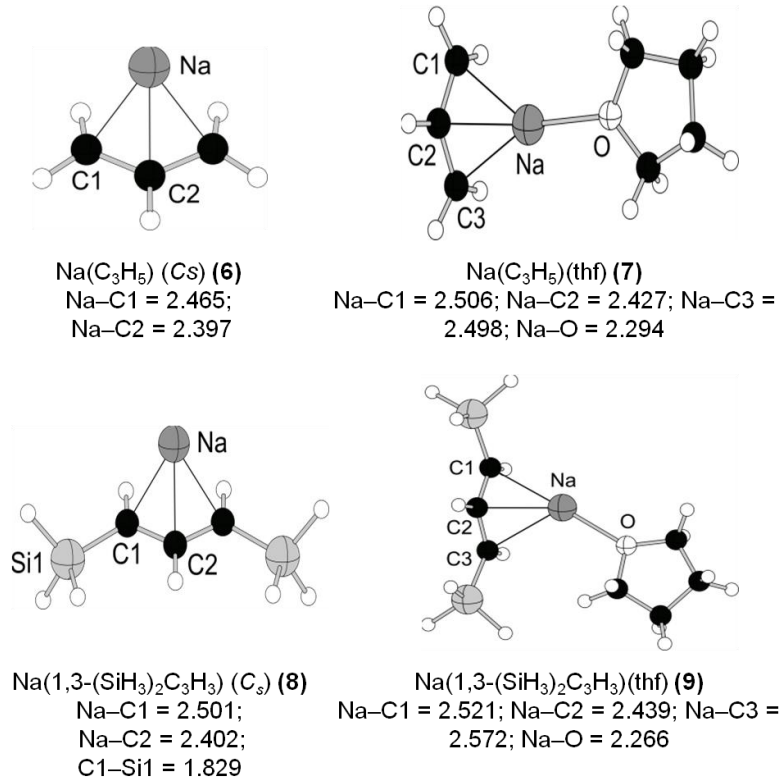

Figure B.3 Optimized structures of allylic species and derivatives.

Complexes 6–9: $Na(C_3H_5)$ (**6**), $Na(C_3H_5)(thf)$ (**7**), $Na(1,3\text{-}(SiH_3)_2C_3H_3)$ (**8**), $Na(1,3\text{-}(SiH_3)_2C_3H_3)(thf)$ (**9**). Although the chemical shift of only the substituted allyl $Na(1,3\text{-}(SiMe_3)_2C_3H_3)(thf)$ is available, several simplified model compounds were examined in order to determine the effect of different substituents on the shift. The parent sodium allyl **6** has a shift that is over 40 ppm downfield of the experimental value, but in contrast to the case with NaCp, the addition of THF (**7**) causes a large upfield shift of over 20 ppm. The bare allyl anion evidently does not dominate the shift to the extent that the Cp anion does.

The profound effect that silyl substitution (using SiH_3 as a computationally less demanding substitute for $SiMe_3$) has on the electronic environment of the allyl anion is evident in compound **8**, whose shift is more than 30 ppm upfield of the unsubstituted allyl, and within

10 ppm of the experimental value for the trimethylsilylated species. Addition of THF to this species in the form of compound **9** again causes an upfield shift, but of just slightly over 5 ppm, putting the calculated shift within 5 ppm of the experimental value for the trimethylsilylated species. It could be that most of the structural features required to model the chemical shift of Na[1,3-$(SiMe_3)_2C_3H_3$] in THF solution have been captured at this level of theory, but as discussed above, it is also possible that the observed chemical shift for the allyl complex is really that of the solvated ion $[Na(thf)_4]^+$.

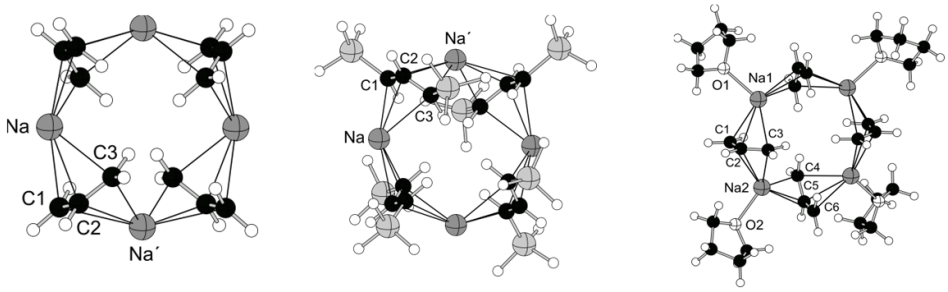

$\{Na(C_3H_5)\}_4$ (D_{2d})
Na–C1 = 2.653; Na–C2 = 2.567; Na–C3 = 2.617

$\{Na(1,3\text{-}(SiH_3)_2C_3H_3)\}_4$ (D_{2d})
Na–C1 = 2.681; Na–C2 = 2.576; Na–C3 = 2.639

{Na(C3H5)(thf)}4 (*C*2)
Na1–C1 = 2.750; Na1–C2 = 2.596; Na1–C3 = 2.633; Na1–O1 = 2.312; Na2–C4 = 2.629; Na1–C2 = 2.616; Na1–C3 = 2.780; Na2–O2 = 2.314

Figure B.4 Optimized structures for allylic tetrameric species.

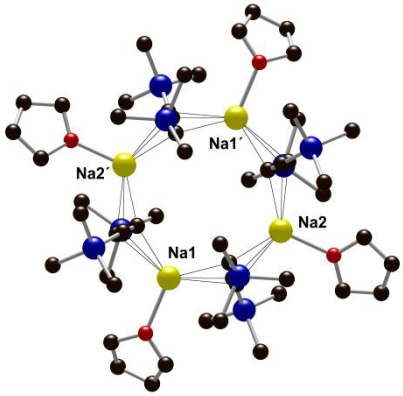

Figure B.5 Crystal structure for $\{Na(1,3\text{-}(SiMe_3)_2C_3H_3)(thf)\}_4$.

Complexes 10–12: $\{Na(C_3H_5)\}_4$ (**10**), $\{Na(1,3\text{-}(SiH_3)_2C_3H_3)\}_4$ (**11**), $\{Na(C_3H_5)(thf)\}_4$ (**12**)

The preceding calculations implicitly assume that the tetrameric solid state $\{Na(1,3\text{-}(SiMe_3)_2C_3H_3)(thf)\}_4$ complex (see Figure B.5) dissociates into monomeric species in solution. Tests of this assumption were made by studying simplified models of the aggregated complex. The smallest model (**10**) removed all substituents from the allyl ligand and the coordinated THF. It minimized to a structure with D_{2d} symmetry, and has a shift that is 14 ppm upfield of the experimental value, evidently reflecting the presence of two negatively charged allyls in the environment of the sodium. These now dominate the shift calculation, and the previously observed effects of silyl substitution and THF addition on the monomeric **6** are muted. There is an additional shift of only 4 ppm upfield with $\{Na(1,3\text{-}(SiH_3)_2C_3H_3)\}_4$ (**11**) and essentially no change (~1 ppm downfield) with $\{Na(C_3H_5)(thf)\}_4$ (**12**). These results are highly suggestive of fragmentation of the tetramer in THF solution.

Indenide Species

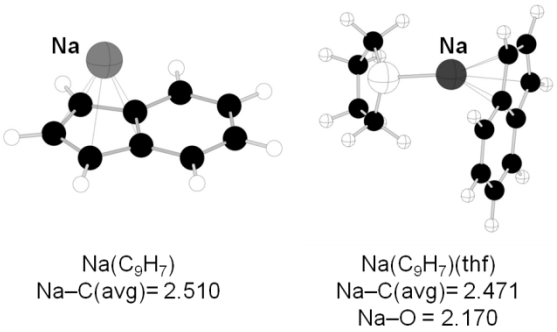

Figure B.6 Optimized structures of sodium indenide species.

Complex 13, 14: $Na(C_9H_7)$ (**13**), $Na(C_9H_7)$ * THF (**14**)

The calculated shift for sodium indenide (**13**) was –45.1, and the addition of a thf to the sodium atom (**14**) moved the shift to –31.35, which is in the same range as the experimental

shift for sodium cyclopentadiene (–33.4 ppm). The implication is that the shift value for this molecule is also dominated by the electron current in the five-membered section of the indenide ring. It is interesting to note that, in the optimized structure, the sodium was not centered over the ring, but was much closer to the carbons bridging the bicyclic ligand. The next logical step in this project would be to synthesize and record the experimental shift of sodium indenide. Further computational, and synthetic work, should then be carried out on sodium complexes with different substituted indenide anions to take advantage of the indenyl ligand's versatility.

Sodium Borate Species

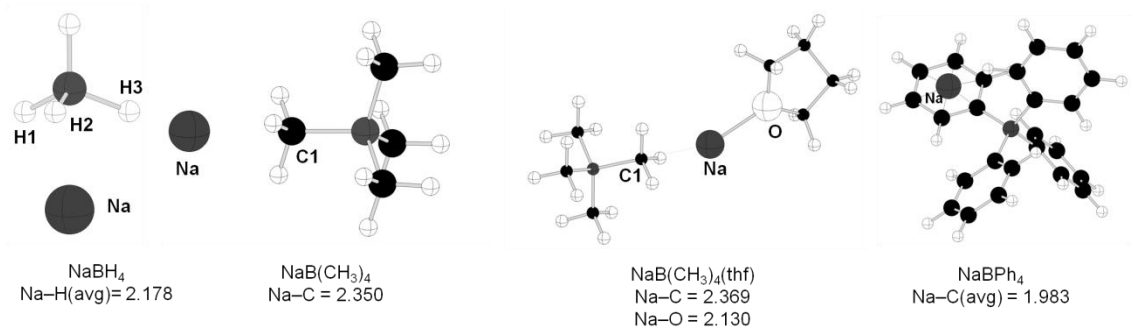

Figure B.7 Optimized structures of sodium borate species.

Complex 15-17: $NaBH_4$(**15**), $NaB(CH_3)_4$ (**16**), $NaB(CH_3)_4$ (**17**), and $Na(BPh_4)$(**18**).

Sodium tetraphenyl borate is an important counter ion in many compounds. The chemical shift for this compound is –8.12 ppm. Two simplified compounds in the same family were also investigated to observe the effects of simplification on the compound. The first, $NaBH_4$ (**15**), showed an adjusted chemical shift of –13.42 ppm. The second, $NaB(CH_3)_4$ (**16**), had a calculated shift of –22.03. The third, $NaB(CH_3)_4$(thf) (**17**), had a calculated shift of –2.19 ppm. Finally, the calculated shift for $NaBPh_4$ (**18**) was –56.45 ppm. The calculated

shift for **15** (Δδ = –5.30 ppm) was much closer to the shift or $NaBPh_4$ than it was expected to be as $NaBH_4$ is not a close approximation of **18**. The calculated shift for **16**, –22.03, is farther away from the experimental value than **15**, indicating that this is still not a good approximation. The calculated shift for **17** (Δδ = 5.93 ppm), as a thf adduct, is as close (in magnitude) to the expected value as **15**. Both of these are likely close to the expected value due to other factors rather than accuracy of the simulation. The calculated shift for **18**, the target molecule, was –56.45 ppm. This diverges from the experimental value of –8.12 ppm by 48.33 ppm, a significant amount. It seems likely that, in solution, the sodium molecule spends most of its time surrounded by thf molecules and not in the influence of the ring current of the BPh_4^- anion. Further evidence for this is the chemical shift of sodium in THF (–5.6 ppm) which is quite close to the experimental shift of –8.12 ppm.

Alkyl Sodium

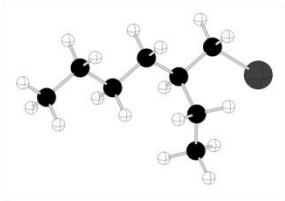

2-ethylhexyl sodium
Na–C = 2.170

Figure B.8 Optimized structure of 2-ethylhexyl sodium.

Complex 19: 2-Ethylhexyl sodium

The calculated value for **19** is –8.0 ppm, while the experimental value is 27 ppm. There are two possible explanations for this. First, the experimental value is not close to the range where organometallic sodium in generally found in ^{23}Na NMR, so it is possible that the

literature value is incorrect. Alkyl sodium complexes tend to be made through experimentally demanding processes and have very short shelf-lives[41], so it is not feasible at this time to reproduce the results. The other possibility is that the compound exists as some sort of dimer or oligomer in solution. Further calculations and experimental work, as well as other examples of alkyl sodium complexes are needed.

Sodide Complex

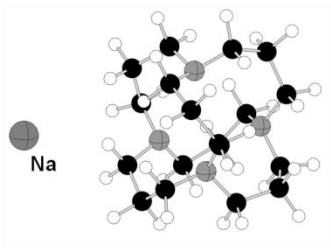

Sodium
Adamantazane
Na–C(avg)= 5.136

Figure B.9 Optimized structure for sodium 3^6adamanzane.

Complex 14: Sodium 3^6Adamanzane Hydride (**20**)

Sodide compounds contain the Na^- anion. Their general shift range is below –60 ppm, far from any other sodium species. The literature value for this compound is from what has been termed "Inverse sodium hydride".[63] A compound where a hydrogen nucleus is encapsulated in a 3^6adamanzane cage was explored; the negatively charged sodide anion is located outside of the cage (Figure B.10[63]). The experimental shift for **20** is –61.0 ppm, and the calculated shift is –73.63 ppm, a difference of –12.6 ppm. This is actually a fairly good first approximation as there is not much computational data on the sodide anion. The addition of some solvent molecules to the calculation would most likely bring the calculated value closer to the experimental value.

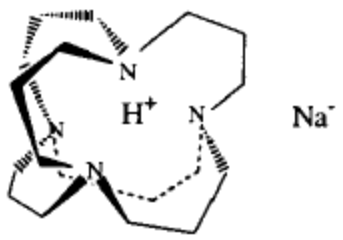

Figure B.10 Structure of inverse sodium hydride.

CONCLUDING REMARKS

Calculation of ^{23}Na NMR shifts with DFT/GIAO methods has been shown to be feasible for a variety of organometallic molecules. The experimental data are still extremely limited, but satisfactory agreement of chemical shift values can be found for cyclopentadienyl and allyl species. With the latter, addition of silyl substituents to model compounds has a large upfield effect on the chemical shifts. It may be possible to distinguish states of aggregation in solution by a comparison of calculated and observed chemical shifts. Much still remains to be understood about the NMR of alkyl sodium complexes and those compounds in which cation–π effects are important, and on the chemical shift in polymetallic aggregates. Future work includes the synthesis of additional compounds, investigation with ^{23}Na NMR, and comparison to computationally determined chemical shifts.

APPENDIX 1: SYNTHESIS OF A BI-METALLIC IONIC LIQUID

Background

Recently work has been published showing the synthesis of imidazolium based ionic liquids with transition metals in both the cation and anion.[64] These ionic salts, $[Cu(Im^{12})_2][CuCl_2]$ and $[Cu(Im^{12})_2][CuBr_2]$, were both solid at room temperature. The chloride salt melted at 73 °C and decomposed at 281 °C while the bromide salt melted at 66 °C and decomposed at 278 °C. It was thought that with a medium or even short length carbon chain, the salt might be liquid at room temperature.

Synthesis

Tetra(methyl imidazolium) copper tetrachlorocuprate(II), $[Cu(mim)_4][CuCl_4]$

$CuCl_2*2H_2O$ (2.36 g, 13.8 mmol) was added to a round bottom flask with methyl imidazole (2.80 g, 34.1 mmol) and approximately 25 mL of acetonitrile. Upon addition of the copper chloride the solution turned the characteristic yellow of $[CuCl_4]^{2-}$. Upon the addition of methylimidazole, the solution turned cobalt blue and became warm to the touch. The solution was allowed to react for several hours under sonication. The solution was dried to obtain a green honey-like solution in quantitative yield.

Results and Discussion

Characterization has not been carried out on this product as yet. However, $[C_7mim][CuCl_4]$ was previously synthesized for electrochemical analysis, but yielded no positive results. The neat ionic liquid contains $CuCl_4^{2-}$ and is yellow. Addition of water causes the solution to turn red due

to the presence of $CuCl_3^-$. However, $[Cu(mim)_4][CuCl_4]$ is a green color. It is assumed this is due to the presence the blue $[Cu(mim)_4]^-$ anion.

REFERENCES

1. Plechkova, Natalia V., and Kenneth R. Seddon. "Applications of ionic liquids in the chemical industry." *Chemical Society Reviews* 37, no. 1 (2008): 123-150.

2. Wasserscheid, Peter, and Wilhelm Keim. "Ionic Liquids—New "Solutions" for Transition Metal Catalysis." *Angewandte Chemie International Edition* 39, no. 21 (2000): 3772-3789.

3. Deng, Ming-Jay, I. Wen Sun, Po-Yu Chen, Jeng-Kuei Chang, and Wen-Ta Tsai. "Electrodeposition behavior of nickel in the water- and air-stable 1-ethyl-3-methylimidazolium-dicyanamide room-temperature ionic liquid." *Electrochimica Acta* 53, no. 19 (2008): 5812-5818.

4. Leong, Tin-Iao, I. Wen Sun, Ming-Jay Deng, Chi-Ming Wu, and Po-Yu Chen. "Electrochemical Study of Copper in the 1-Ethyl-3-Methylimidazolium Dicyanamide Room Temperature Ionic Liquid." *Journal of The Electrochemical Society* 155, no. 4 (2008): F55-F60.

5. Zhuang, Ding-Xuan, Ming-Jay Deng, Po-Yu Chen, and I. Wen Sun. "Electrochemistry of Manganese in the Hydrophilic N-Butyl-N-methylpyrrolidinium Dicyanamide Room-Temperature Ionic Liquid." *Journal of The Electrochemical Society* 155, no. 9 (2008): D575-D579.

6. Welton, Thomas. "Room-Temperature Ionic Liquids. Solvents for Synthesis and Catalysis." *Chemical Reviews* 99, no. 8 (1999): 2071-2084.

7. Newington, Ian, Juan M. Perez-Arlandis, and Tom Welton. "Ionic Liquids as Designer Solvents for Nucleophilic Aromatic Substitutions." *Organic Letters* 9, no. 25 (2007): 5247-5250.

8. Plechkova, N.V., and K.R. Seddon. "Ionic Liquids: designer solvents for green chemistry." In *Methods and Reagents for Green Chemistry: An Introduction*, edited by A. Perosa, F. Zecchini and P. Tundo. Hoboken, NJ: John Wiley and Sons, 2007.

9. Abbott, Andrew P., Glen Capper, David L. Davies, and Raymond Rasheed. "Ionic Liquids Based upon Metal Halide/Substituted Quaternary Ammonium Salt Mixtures." *Inorganic Chemistry* 43, no. 11 (2004): 3447-3452.

10. Binnemans, Koen. "Lanthanides and Actinides in Ionic Liquids." *Chemical Reviews* 107, no. 6 (2007): 2592-2614.

11. Gale, R. J., B. Gilbert, and R. A. Osteryoung. "Electrochemical and spectral investigations of nickel(II) ion equilibriums in room-temperature chloroaluminate solvents." *Inorganic Chemistry* 18, no. 10 (1979): 2723-2725.

12. Oye, Harald A., and Dieter Gruen. "Cobalt(II) Species in Fused Chloride Solvents." *Inorganic Chemistry* 4, no. 8 (1965): 1173-1180.

13. Bowlas, Christopher J., Duncan W. Bruce, and Kenneth R. Seddon. "Liquid-crystalline ionic liquids." *Chemical Communications*, no. 14 (1996): 1625-1626.

14. Meredith, M. Brett, C. Heather McMillen, Jonathan T. Goodman, and Timothy P. Hanusa. "Ambient temperature imidazolium-based ionic liquids with tetrachloronickelate(II) anions." *Polyhedron* 28, no. 12 (2009): 2355-2358.

15. Ni, Yonghong, Jun Li, Lina Jin, Jun Xia, Jianming Hong, and Kaiming Liao. "Co_2P nanostructures constructed by nanorods: hydrothermal synthesis and applications in the removal of heavy metal ions." *New Journal of Chemistry* 33, no. 10 (2009): 2055-2059.

16. Yao, Zhiwei, Aimin Zhu, C. T. Au, and Chuan Shi. "Redox Properties of Cobalt Nitrides for NO Dissociation and Reduction." *Catalysis Letters* 130 (2009): 63-71.

17. De La Cruz, W., O. Cibtreras, G. Soto, and E. Perez-Tijerina. "Cobalt nitride films produced by reactive pulsed laser deposition." *Revista Mexicana De Fisca* 52, no. 5 (2006): 409–412.

18. Hyeon, T. "Chemical synthesis of magnetic nanoparticles." *Chemical Communications (Cambridge, United Kingdom)*, no. 8 (2003): 927-934.

19. Meredith, M. Brett. Vanderbilt University, 2004.

20. Wilkes, John S., Joseph A. Levisky, Robert A. Wilson, and Charles L. Hussey. "Dialkylimidazolium chloroaluminate melts: a new class of room-temperature ionic liquids for electrochemistry, spectroscopy and synthesis." *Inorganic Chemistry* 21, no. 3 (1982): 1263-1264.

21. Sanders, John R., Edmund H. Ward, and Charles L. Hussey. "Aluminum Bromide-1-Methyl-3-Ethylimidazolium Bromide Ionic Liquids." *Journal of The Electrochemical Society* 133, no. 2 (1986): 325-330.

22. Huddleston, Jonathan G., Ann E. Visser, W. Matthew Reichert, Heather D. Willauer, Grant A. Broker, and Robin D. Rogers. "Characterization and comparison of hydrophilic and hydrophobic room temperature ionic liquids incorporating the imidazolium cation." *Green Chemistry* 3, no. 4 (2001): 156-164.

23. Branco, Luís C., João N. Rosa, Joaquim J. Moura Ramos, and Carlos A. M. Afonso. "Preparation and Characterization of New Room Temperature Ionic Liquids." *Chemistry – A European Journal* 8, no. 16 (2002): 3671–3677.

24. Mingos, D. Michael P., and Andrew L. Rohl. "Size and shape characteristics of inorganic molecules and ions and their relevance to molecular packing

problems." *Journal of the Chemical Society, Dalton Transactions*, no. 12 (1991): 3419-3425.

25. Jin, Hui, Bernie O'Hare, Jing Dong, Sergei Arzhantsev, Gary A. Baker, James F. Wishart, Alan J. Benesi, and Mark Maroncelli. "Physical Properties of Ionic Liquids Consisting of the 1-Butyl-3-Methylimidazolium Cation with Various Anions and the Bis(trifluoromethylsulfonyl)imide Anion with Various Cations." *The Journal of Physical Chemistry B* 112, no. 1 (2007): 81-92.

26. Aronsson, B., T. Lundstrom, and S. Rundquist. *Borides, Silicides and Phosphides*. New York, NY: Wiley, 1965.

27. McAuliffe, C.A. *Phosphine, Arsine, and Stilbine Complexes of the Transition Elements*. Amsterdam: Elsevier, 1979.

28. Liu, Yang, Lihong Shi, Meijia Wang, Zhiying Li, Hongtao Liu, and Jinghong Li. "A novel room temperature ionic liquid sol-gel matrix for amperometric biosensor application." *Green Chemistry* 7, no. 9 (2005): 655-658.

29. Neouze, Marie-Alexandra, Jean Le Bideau, Fabrice Leroux, and Andre Vioux. "A route to heat resistant solid membranes with performances of liquid electrolytes." *Chemical Communications*, no. 8 (2005): 1082-1084.

30. Gobet, Mallory, Corinne Rondeau-Mouro, Solange Buchin, Jean-Luc Le Quéré, Elisabeth Guichard, Loïc Foucat, and Céline Moreau. "Distribution and mobility of phosphates and sodium ions in cheese by solid-state ^{31}P and double-quantum filtered ^{23}Na NMR spectroscopy." *Magnetic Resonance in Chemistry* 48, no. 4 (2010): 297-303.

31. Schepkin, Victor D., Kuei C. Lee, Kyle Kuszpit, Mukilan Muthuswami, Timothy D. Johnson, Thomas L. Chenevert, Alnawaz Rehemtulla, and Brian D. Ross. "Proton and sodium MRI assessment of emerging tumor chemotherapeutic resistance." *NMR in Biomedicine* 19, no. 8 (2006): 1035-1042.

32. Dye, J.L., and A.S. Ellaboudy. "Solid State NMR of Quadrupolar Nuclei." In *Modern NMR Techniques and Their Application in Chemistry*, edited by Popov and Hallenga, 217-322. Boca Raton, FL: CRC Press, 1991.

33. Willans, Mathew J., and Robert W. Schurko. "A Solid-State NMR and ab Initio Study of Sodium Metallocenes." *The Journal of Physical Chemistry B* 107, no. 22 (2003): 5144-5161.

34. Charpentier, Thibault, Simona Ispas, Mickael Profeta, Francesco Mauri, and Chris J. Pickard. "First-Principles Calculation of ^{17}O, ^{29}Si, and ^{23}Na NMR Spectra of Sodium Silicate Crystals and Glasses." *The Journal of Physical Chemistry B* 108, no. 13 (2004): 4147-4161.

35. Erlich, Ronald H., and Alexander I. Popov. "Spectroscopic studies of ionic solvation. X. Study of the solvation of sodium ions in nonaqueous solvents by

sodium-23 nuclear magnetic resonance." *Journal of the American Chemical Society* 93, no. 22 (1971): 5620-5623.

36. Schroeder, G., B. Gierczyk, B. Brzezinski, B. Rózalski, F. Bartl, G. Zundel, J. Sosnicki, and E. Grech. "23Na NMR and FT-IR studies of sodium complexes with the ionophore lasalocid in solution." *Journal of Molecular Structure* 516, no. 1 (2000): 91-98.

37. Gutmann, Viktor. "Solvent effects on the reactivities of organometallic compounds." *Coordination Chemistry Reviews* 18, no. 2 (1976): 225-255.

38. McMillen, C. Heather, Cameron K. Gren, Timothy P. Hanusa, and Arnold L. Rheingold. "A tetrameric allyl complex of sodium, and computational modeling of the ^{23}Na-allyl chemical shift." *Inorganica Chimica Acta* 364 (2010): 61-68.

39. Hill, Michael S., and Peter B. Hitchcock. "Sodium and potassium derivatives of diphenyl(trimethylsilyl)methane." *Journal of Organometallic Chemistry* 664, no. 1-2 (2002): 182-187.

40. Moser, Arvin, Glenn P. A. Yap, and Christian Detellier. "Concurrent insertion of cationic guest and solvent molecules in molecular receptors. Co-complexation of the sodium cation and acetonitrile by a calix[4]arene tetra-acetamide." *Journal of the Chemical Society, Dalton Transactions*, no. 3 (2002): 428-434.

41. Pakuro, N. I., A. A. Arest-Yakubovich, L. V. Shcheglova, P. V. Petrovsky, and L. A. Chekulaeva. "NMR spectra of a hydrocarbon-soluble organosodium compound and its lithium analogs." *Russian Chemical Bulletin* 45, no. 4 (1996): 838-840.

42. Paquette, Leo A., Walter Bauer, Mark R. Sivik, Michael Buehl, Martin Feigel, and Paul v R. Schleyer. "Structure of lithium isodicyclopentadienide and lithium cyclopentadienide in tetrahydrofuran solution. A combined NMR, IGLO, and MNDO study." *Journal of the American Chemical Society* 112, no. 24 (1990): 8776-8789.

43. Johnels, Dan, Arne Boman, and Ulf Edlund. "^{7}Li solid-state NMR spectroscopic study of cyclopentadienyllithium complexes." *Magnetic Resonance in Chemistry* 36, no. S1 (1998): S151-S156.

44. Gren, Cameron K., Timothy P. Hanusa, and Arnold L. Rheingold. "Threefold Cation π Bonding in Trimethylsilylated Allyl Complexes." *Organometallics* 26, no. 7 (2007): 1643-1649.

45. Plieger, Paul G., Kevin D. John, Timothy S. Keizer, T. Mark McCleskey, Anthony K. Burrell, and Richard L. Martin. "Predicting ^{9}Be Nuclear Magnetic Resonance Chemical Shielding Tensors Utilizing Density Functional Theory." *Journal of the American Chemical Society* 126, no. 44 (2004): 14651-14658.

46. White, Rosemary E., and Timothy P. Hanusa. "Prediction of ^{89}Y NMR Chemical Shifts in Organometallic Complexes with Density Functional Theory." *Organometallics* 25, no. 23 (2006): 5621-5630.

47. Koller, Hubert, Guenter Engelhardt, Arno P. M. Kentgens, and Joachim Sauer. "23Na NMR Spectroscopy of Solids: Interpretation of Quadrupole Interaction Parameters and Chemical Shifts." *The Journal of Physical Chemistry* 98, no. 6 (1994): 1544-1551.

48. Gaussian 03 Version Revision E.01. Gaussian, Inc, Wallingford, CT.

49. Barfield, Michael, and Paul Fagerness. "Density Functional Theory/GIAO Studies of the ^{13}C, ^{15}N, and ^{1}H NMR Chemical Shifts in Aminopyrimidines and Aminobenzenes: Relationships to Electron Densities and Amine Group Orientations." *Journal of the American Chemical Society* 119, no. 37 (1997): 8699-8711.

50. Perdew, John P., Kieron Burke, and Matthias Ernzerhof. "Generalized Gradient Approximation Made Simple." *Physical Review Letters* 77, no. 18 (1996): 3865.

51. Helgaker, Trygve, Michal Jaszunski, and Kenneth Ruud. "Ab Initio Methods for the Calculation of NMR Shielding and Indirect Spin-Spin Coupling Constants." *Chemical Reviews* 99, no. 1 (1998): 293-352.

52. Kanda, Takahiro, Mitsuo Ibi, Ken-ichi Mochizuki, and Shinzi Kato. "The First Isolation and Structural Analysis of Chalcogenocarboxylato Samarium Complexes, $[(RCOS)_3Sm(thf)_2]$ and $[Na(thf)_4][Sm(RCSS)_4]$; The Alkali Metal Salt-Like Reaction and the Insertion Reaction of Imine to the Sm-S Bond." *Chemistry Letters* 27, no. 9 (1998): 957-958.

53. Paschina, G., G. Piccaluga, G. Pinna, and M. Magini. "X-ray investigation of Co---Cl bonding in a concentrated aqueous solution of $CoCl_2$ and LiCl." *Chemical Physics Letters* 98, no. 2 (1983): 157-161.

54. Ohtomo, Norio, and Kiyoshi Arakawa. "Neutron Diffraction Study of Aqueous Ionic Solutions. II. Aqueous Solutions of Sodium Chloride an Potassium Chloride." *Bulletin of the Chemical Society of Japan* 53, no. 7 (1980): 1789-1794.

55. Kameda, Yasuo, Kentaro Sugawara, Takeshi Usuki, and Osamu Uemura. "Hydration Structure of Na+ in Concentrated Aqueous Solutions." *Bulletin of the Chemical Society of Japan* 71, no. 12 (1998): 2769-2776.

56. Waizumi, Kenji, Hideki Masuda, and Nobuhiro Fukushima. "Structural rigidity of first hydration spheres of Na^+ and Ca_2^+ in cluster models. Full geometry optimizations of $[M(H_2O)_6]_n^+$, $[M(H_2O)_6...H_2O]_n^+$ and $[M(H_2O)_6...Cl]_{(n-1)}^+$ (M = Na and Ca, n = 1 for Na and 2 for Ca) by density functional calculations." *Inorganica Chimica Acta* 209, no. 2 (1993): 207-211.

57. Liu, Yun, John Tossell, and Hanna Nekvasil. "A theoretical study of structural factors correlated with ^{23}Na NMR parameters." *American Mineralogist* 89 (2004): 1314-1322.

58. Kutzelnigg, W., and U. Fleischer, eds. *NMR Basic Principles and Progress*. Edited by Diehl, Fluck, Gunther, Kosfelt and Seelig. Vol. 23. Berlin: Springer-Verlag, 1991.

59. Forsyth, David A., and Albert B. Sebag. "Computed ^{13}C NMR Chemical Shifts via Empirically Scaled GIAO Shieldings and Molecular Mechanics Geometries. Conformation and Configuration from ^{13}C Shifts." *Journal of the American Chemical Society* 119, no. 40 (1997): 9483-9494.

60. Detellier, Christian, André Gerstmans, and Pierre Laszlo. "Sodium-23 NMR study of preferential Na+ solvation in diethylenetriamine-tetrahydrofuran mixture." *Inorganic and Nuclear Chemistry Letters* 15, no. 2 (1979): 93-97.

61. Delville, Alfred, Christian Detellier, Andre Gerstmans, and Pierre Laszlo. "Chelation of the sodium cation by polyamines: a novel approach to preferential solvation, and to the understanding of sodium-23 chemical shifts and quadrupolar coupling constants." *Journal of the American Chemical Society* 102, no. 21 (1980): 6558-6559.

62. Delville, Alfred, Christian Detellier, André Gerstmans, and Pierre Laszlo. "The theoretical interpretation of sodium-23 NMR chemical shifts and quadrupolar coupling constants, as supported by new experimental evidence." *Journal of Magnetic Resonance (1969)* 42, no. 1 (1981): 14-27.

63. Redko, Mikhail Y., Mircea Vlassa, James E. Jackson, Andrzej W. Misiolek, Rui H. Huang, and James L. Dye. ""Inverse Sodium Hydride": A Crystalline Salt that Contains H^+ and Na^-." *Journal of the American Chemical Society* 124, no. 21 (2002): 5928-5929.

64. Stricker, Marion, Thomas Linder, Benjamin Oelkers, and Jorg Sundermeyer. "Cu(i)/(ii) based catalytic ionic liquids, their metallo-laminate solid state structures and catalytic activities in oxidative methanol carbonylation." *Green Chemistry* 12, no. 9: 1589-1598.